Modeling Tropical Pacific Sea Surface Temperature with Satellite-Derived Solar Radiative Forcing*

RICHARD SEAGER† AND M. BENNO BLUMENTHAL

Lamont-Doherty Earth Observatory of Columbia University, Palisades, New York

(Manuscript received 23 December 1993, in final form 4 April 1994)

ABSTRACT

Two independent datasets for the solar radiation at the surface derived from satellites are compared. The data derived from the Earth Radiation Budget Experiment (ERBE) is for the net solar radiation at the surface whereas the International Satellite Cloud Climatology Project (ISCCP) data is for the downward flux only and was corrected with a space- and time-varying albedo. The ISCCP net flux is at all times higher than the ERBE flux. The difference can be divided into an offset that decreases with latitude and another component that correlates with high tropical cloud cover. With this latter exception the two datasets provide spatial patterns of solar flux that are very similar.

A tropical Pacific Ocean model is forced with these two datasets and observed climatological winds. The upward heat flux is parameterized taking into account separately the longwave radiative, latent, and sensible heat fluxes. Best fit values for the uncertain parameters are found using an optimization procedure that seeks to minimize the difference between model and observed SST by varying the parameters within a reasonable range of uncertainty. The SST field the model produces with the best fit parameters is the best the model can do. If the differences between the model and data are larger than can be accounted for by remaining uncertainties in the heat flux parameterization and forcing data then the ocean model must be held to be at fault. Using this method of analysis, a fundamental model fault is identified. Inadequate treatment of mixed layer/entrainment processes in upwelling regions of the eastern tropical Pacific leads to a large and seasonally varying error in the model SST. Elsewhere the model SST is insufficiently different from observed to be able to identify model errors. Some implications for ocean modeling of the seasonal cycle are discussed.

1. Introduction

Recent advances in the modeling and prediction of tropical climate have made accurate simulation of sea surface temperature (SST) a matter of considerable importance. The SST is the only ocean property that the atmosphere sees and hence is crucial in phenomena involving atmosphere–ocean interaction. The El Niño–Southern Oscillation (ENSO), Asian monsoon variability, and droughts in Africa and Brazil are all linked, or hypothesized to be linked, to variability of tropical SST (Zebiak and Cane 1987; Palmer et al. 1992; Moura and Shukla 1981). Through teleconnections to higher latitudes, weather and climate variability worldwide responds to variations of tropical SST. Numerous modeling studies have found the extratropical winter hemisphere to be particularly sensitive to relatively small SST anomalies in the western Pacific (e.g., Geisler et al. 1985).

The routine forecasting of ENSO conducted at the Lamont-Doherty Earth Observatory uses an anomaly model that calculates SST departures from the seasonal cycle. While this has afforded significant progress (see Cane 1991 for a review) it has its limitations. For example, the real atmosphere responds to total, rather than anomalous, SST and, though the forecast model attempts to account for this, specifying the climatology may eliminate certain forms of coupled behavior. Further, ENSO variability on timescales of decades may be more usefully viewed as shifts in the tropical Pacific climate rather than as departures from a time invariant climatology. That is also true of the basin-scale modes of SST variability that have been hypothesized as being related to African and Brazilian droughts (e.g., Moura and Shukla 1981). If we are to understand (and ultimately predict) these phenomena, it is clear that accurate models capable of modeling total, rather than anomalous, SST are required.

Seager et al. (1988, hereafter SZC) and Seager (1989) presented attempts to model the climatology and variability of tropical Pacific SST using a realistic surface heat flux formulation. Previous attempts had used either a relaxation to climatology [e.g., Han (1984) and

---

* Contribution Number 5188 of Lamont-Doherty Earth Observatory.

† NOAA Program in Climate and Global Change Visiting Postdoctoral Fellow.

Corresponding author address: Dr. Richard Seager, Lamont-Doherty Earth Observatory, Palisades, NY 10964.

© 1994 American Meteorological Society

first suggested by Haney (1971)] or idealized heat fluxes [e.g., Latif (1987) and Philander and Siegel (1985), whose formulation was later adopted by Harrison (1991)]. SZC used the linear, reduced gravity, ocean model used at L-DEO for ENSO prediction but with a new parameterization of the temperature of the water upwelled into the model mixed layer. They used Reed's (1977) solar radiation formula, which parameterizes the downward solar radiation at the surface in terms of cloud cover, latitude, and time of year. Weare et al.'s (1980) surface observed cloud cover was used. The latent heat flux was computed using the standard bulk formula but assuming that the air humidity was a fixed proportion of the saturation humidity evaluated at the modeled SST. The longwave and sensible fluxes were combined into a simple cooling that was linear in the SST.

Adoption of this surface heat flux formulation avoided the need to specify the air humidity and air temperature. It had been noticed that the air temperature closely parallels the SST and that the air humidity also varies approximately linearly in SST. Away from coasts it is the SST that dominates this relationship; that is, the air temperature and humidity track the SST because it is they that adjust to the SST and not the other way around. Hence SZC argued, and later Gent (1991) concurred, that to specify these quantities for the purposes of surface flux calculation puts in a great deal of the answer by providing the model with information on the SST. In effect it includes a relaxation to the observed SST, which makes interpretation of model results and assessment of model failings difficult.

Since then Gordon and Corry (1991) and Miller et al. (1992) have presented SST simulations that both give reasonable results. However, Gordon and Corry force their model with fluxes derived from the U.K. Meteorological Office atmospheric General Circulation Model (GCM) but point out that a good SST simulation nonetheless requires a term relaxing the model SST to observed. This term can be locally very large. Miller et al. used the complete bulk formula and imposed observed air temperature and humidity. In contrast, in this paper we will continue our efforts to model tropical SST in the absence of any such constraints, allowing maximum freedom of the model to determine its own SST.

Blumenthal and Cane (1989, hereafter BC) introduced a way of accounting for the uncertainties in the parameters that needed to be specified in the calculations of SZC. Quantities such as the exchange coefficient, the proportionality constant between saturation humidity and air humidity, the coefficient reducing the solar radiation to account for cloud cover, and several others are all uncertain. Blumenthal and Cane assumed a priori values and uncertainties for all these parameters. They then computed the residual heat flux that would be required to bring the model SST into agreement with observed SST at each time step. They next performed an optimization of the heat flux calculation by allowing the specified parameters to vary within the range of their assumed uncertainty in order to minimize the residual heat flux. This provides the set of parameters within the range of physical validity that provides the best fit between model and observed SST.

The remaining uncertainty in the calculation is introduced by errors in the forcing data (winds, cloud cover) and model errors. If the best fit SST differs from the observed SST by less than can be accounted for by errors in the input data, then it is not possible to unambiguously state that the model is wrong, even though it almost certainly is. In this case the errors in the forcing data are large enough to account for all the differences between the model and data. Blumenthal and Cane show that this was in fact the case for the tropical Pacific. However in the Atlantic the model was shown, unambiguously, to be incapable of modeling SST near the African coasts. This was assumed to be related to errors in the latent heat flux formula in a region where the atmosphere is not in equilibrium with the SST and also to errors in the treatment of upwelling and possibly eastern boundary currents.

For the Pacific this was an enlightening, but rather unsatisfactory, state of affairs. We were sure the model was wrong in important ways but were unable to either prove this or show where the problems lay. Blumenthal and Cane concluded further advances would have to await improved forcing data. It was hoped that the advent of satellite-derived solar radiation would provide the next advance. Since then two global surface solar radiation datasets have become available. The first is derived from the International Satellite Cloud Climatology Project (ISCCP) (Rossow and Schiffer 1991) and the second from the Earth Radiation Budget Experiment (ERBE) data as described by Li and Leighton (1993).

Here we replace the bulk formula estimated solar radiation of SZC and BC with the satellite observations in model-based calculations of climatological tropical Pacific SST. We also use a more general surface flux formulation that uses bulk formulas for the latent, sensible, and longwave fluxes. As in the preceding papers mentioned above, we exclude specification of parameters such as air temperature and humidity over which the ocean has a strong influence. We then perform an optimization calculation to provide a set of best fit parameters and obtain the best possible SST given this model and this set of forcing data.

We will use these results to draw conclusions on the adequacy of the dynamical model, the adequacy of the forcing data, and the method of computing surface fluxes in ocean models. In conclusion we will make some statements about how close we now are to the goal of accurate simulation of SST in the absence of specification of unjustified quantities or relaxation to climatology terms. In this paper we focus solely on the

climatology leaving simulation of interannual variability for a later study.

2. Satellite-derived surface solar radiation data

We use two independent satellite-derived surface solar radiation datasets. The first uses data from the ISCCP (Rossow and Schiffer 1991). ISCCP uses data from a wide complement of operational weather satellites. The data provides high temporal and spatial resolution measurements of required atmospheric quantities such as cloud fraction, optical thickness, and temperature and pressure at cloud top, together with measurements of ozone and aerosol abundance and information on the underlying surface. Bishop and Rossow (1991) used ISCCP data as input in the solar radiative transfer scheme that is operational in the Goddard Institute for Space Studies GCM to derive the downward solar radiation at the surface. They then develop a faster and simpler scheme for computing surface solar radiation that also uses ISCCP data as input and calibrated this model against the complete radiative transfer scheme. They show the discrepancies to be within 6 W m^{-2} over the oceans. The results of the fast scheme were compared to surface observations at six midlatitude ocean weather stations and one continental station, and errors were reported to be typically less than 10 W m^{-2}. A global dataset has been compiled using the fast algorithm for the period beginning in July 1983.

To get the net solar radiation at the surface the downward irradiance needs to be corrected for the fraction that is reflected. We use the formula of Cox and Munk (1956) for the ocean albedo, which relates the albedo to the solar zenith angle and also, weakly, to the wind speed. A constant 5 m s^{-1} wind speed is assumed. The net solar radiation at the surface is shown in Fig. 1 for March and September climatologies of the period from January 1985 to December 1989. This period was used to conform to the more limited time coverage of the ERBE data and ensures the comparison is not affected by the months for which there is no ERBE data. March and September were chosen to illustrate the extremes of the tropical Pacific annual cycle. It should be noted that five years is a relatively short time over which to establish a climatology. The period includes a modest warm event and a cold event and hence does capture an entire ENSO cycle. All the work reported here will have to be updated as satellite data for longer periods becomes available.

[Since this work was completed, a new ISCCP dataset has become available. The new data corrects for two satellite calibration errors that are in the original data (Bishop and Rossow 1994, personal communication). However, the data for February 1985 to October 1988 inclusive were not adjusted. In the work reported here we compile a climatology over the period January 1985 to December 1989. Comparison of the revised climatology for this period with the climatology used here reveals the latter to be 2–6 W m^{-2} higher over the tropical Pacific region. The upper limit occurs in the cloudiest regions. Such a small (1%–3% of the downward flux), and relatively uniform, change would have minor effect on the modeled SST.]

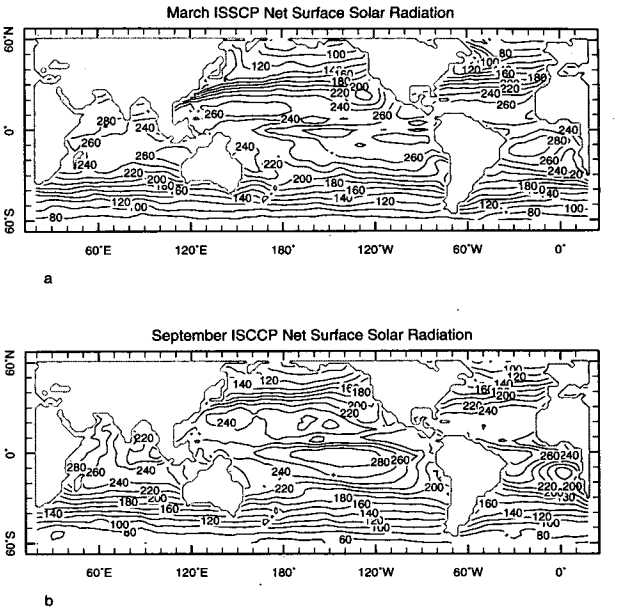

FIG. 1. International Satellite Cloud Climatology Project net surface solar radiation in W m^{-2} for (a) March and (b) September.

The other dataset is the surface solar radiation budget derived from the ERBE data as described by Li and Leighton (1993). ERBE combines data from the Earth Radiation Budget Satellite and the polar orbiting *NOAA-9* and *NOAA-10* satellites. Li et al. (1993b) showed, on the basis of detailed radiative transfer calculations, that it was possible to derive the absorbed surface solar radiation from the satellite measured reflected solar at the top of the atmosphere using simple linear relationships dependent on the solar zenith angle and atmospheric precipitable water content. The latter was obtained from European Centre for Medium-Range Weather Forecasts global analyses. Li and Leighton (1993) used this method to produce a global dataset of surface absorbed solar radiation for the years 1985 to 1989. The climatological averages for this period for March and September are shown in Fig. 2.

These two datasets are entirely independent of one another. ISCCP uses narrowband data from the two NOAA satellites whereas ERBE uses broadband data from the same satellites. Also ISCCP includes data from many satellites not included in ERBE, whereas the Earth Radiation Budget Satellite used in ERBE was not included in ISCCP. Moreover the algorithms for obtaining the surface solar radiation are quite different: the ERBE data depends only on the solar spectrum, whereas the ISCCP data depends on radiative transfer

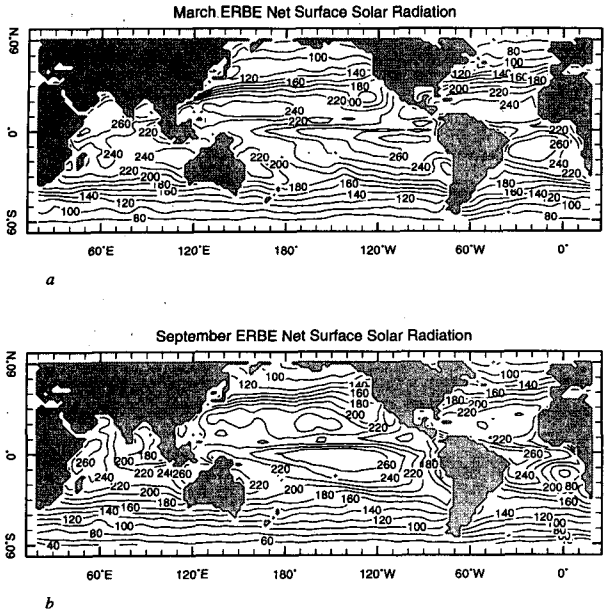

FIG. 2. Earth Radiation Budget Experiment net surface solar radiation in W m^{-2} for (a) March and (b) September.

calculations that use atmospheric profile information derived from the solar and longwave spectrums. It is hence instructive to compare the two. A month to month comparison reveals that the differences are largely independent of time and, in Fig. 3, we show the annual mean difference, ISCCP minus ERBE.

The overwhelming feature is that the ERBE data gives values for absorbed solar radiation that are 10–30 W m^{-2} less than the ISCCP values throughout the Tropics. Differences at higher latitudes tend to be less and the differences are slightly smaller in July than in January. The larger ISCCP values are found despite using a modified form of the Cox and Munk albedo formula giving an albedo of 0.04 for an overhead sun that reduces the radiation absorbed. The ERBE data never gives absorbed solar radiation that is significantly higher than the ISCCP data. These differences should be considered in light of stated goal of the World Climate Research Program Surface Radiation Budget (SRB) project to provide global SRB climatologies to an accuracy of 10 W m^{-2} (Suttles and Ohring 1986).

For the ISCCP data Bishop and Rossow (1991) cite an algorithm error of 6–9 W m^{-2} for daily average downward solar radiation as compared to values calculated by a full radiative transfer model. They compared their computed values to observed values at six ocean weather stations in temperate latitudes and a continental station in Wisconsin, and again showed an accuracy of better than 9 W m^{-2}. Li et al. (1993a) also provide a comparison of their SRB with ground measurements. The measurements they chose were from towers located in Boulder, Colorado, and Saskatoon, Saskatchewan, Canada. Among some not insignificant scatter they showed the net surface solar radiation, as derived from satellite data in conjunction with their algorithm, differed in the mean from the observed values by less than 3 W m^{-2}. Hence, although a typical single measurement may be in error by several percent, the averages of many measurements, such as is used to get a monthly mean, should be small. Using monthly mean values of precipitable water, cosine of zenith angle, and solar flux at the top of the atmosphere, as Li and Leighton (1993) did to compile the global dataset used here, still left the error below 6 W m^{-2}. Since the ISCCP dataset is for downward solar radiation and the ERBE data is for net solar radiation, and also since none were calibrated at the same location, it is difficult to cross-validate these comparisons. It is noteworthy that the largest differences between the datasets was found in the Tropics where neither dataset was calibrated. Comparison of the datasets with ground truth tropical data seems a priority for the future.

In the Tropics the maximum difference occurs in areas of significant high cloud cover where the ISCCP values can exceed the ERBE values by over 20 W m^{-2}. With the exception of these areas the two datasets give very similar spatial patterns of net surface solar radiation. The fact that the differences are explained by a clear, latitudinally dependent offset and a cloud cover correction is encouraging and suggests that reconciling the two estimates in the future will not be difficult.

3. Model description

The tropical Pacific Ocean model used here consists of an ocean model combined with a surface mixed-layer model that calculates dynamical tendencies of SST and a model for the surface heat flux. We will describe each component in turn.

a. Ocean model

The dynamical ocean model used has been described extensively in the literature (SZC, BC) and we will offer only a brief reminder of its structure here referring the reader to other sources for details. The model is a single vertical mode model for linear motions on an equatorial β plane subject to a low-frequency approx-

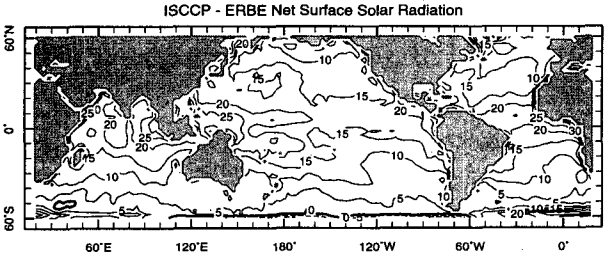

FIG. 3. Annual mean difference, ISCCP minus ERBE, net surface solar radiation in W m^{-2}.

imation (Cane 1979). The model is hence identical to that of SZC, who, however, described it in terms of the reduced gravity formalism. The mode has an equivalent depth of 86 cm and phase speed of 2.9 m s^{-1}, which corresponds in the reduced gravity formalism to an upper-layer depth of 150 m. The relatively small equivalent depth in some ways compensates for the absence of higher-order modes of smaller equivalent depth (Cane 1984). The model basin extends from 30°N to 30°S and, unlike SZC, includes an approximation to the coastline geometry. The model is forced with The Florida State University (FSU) winds (Goldenberg and O'Brien 1981) and the method of solution is the combined analytical–numerical technique of Cane and Patton (1984).

The model incorporates a well-mixed surface layer of constant 50-m depth. Model currents are forced in two ways: directly by the wind forcing and by the pressure gradients that are established in response to the winds. The directly wind-forced component is separated out and assumed to be concentrated in the surface layer. This is designed to account for the surface intensification of the currents. The total currents in the surface layer are determined by the addition of this directly wind-forced component and the nearly geostrophic component forced by pressure gradients. The formal separation of the wind-forced current into the mixed layer is given in SZC. Simulating the intensity of the surface currents is essential for SST determination.

The SST is calculated using the fully nonlinear temperature equation assuming that temperature is constant throughout the mixed layer depth. Horizontal advection is computed using upwind differencing. If water is entrained into the mixed layer (which, since the depth is constant, occurs whenever there is divergence in the surface layer), its temperature is calculated using a parameterization for the temperature of subsurface water in terms of thermocline depth. The parameterization is based on the observational data of Levitus (1982) and is described in SZC and also in BC.

b. *Surface heat flux model*

The total surface heat flux, Q, through the air–sea interface is given by

$$Q = Q_{\text{solar}} - Q_{\text{LH}} - Q_{\text{SH}} - Q_{\text{LW}}, \qquad (1)$$

where Q_{solar} is the absorbed solar radiation, Q_{LH} is the latent heat flux, Q_{SH} is the sensible heat flux, and Q_{LW} is the net longwave radiation loss from the ocean surface.

SZC, Seager (1989), and BC used Reed's (1977) bulk formula for the downward solar radiation, which computes a clear sky flux in terms of latitude and time of year and then corrects this for cloud cover. They used the Weare et al. (1980) surface-observed cloud data and corrected the downward solar with a constant surface albedo (0.06) to get the absorbed solar radiation. In this study we use this form for a benchmark case only. We then replace the bulk formula with the satellite-derived solar radiation data described in the preceding section.

The latent heat flux is modeled using the standard bulk formula:

$$Q_{\text{LH}} = \rho_a c_E L v (q_s - q_a), \qquad (2)$$

where ρ_a is the air density, c_E is an exchange coefficient, L is the latent heat of evaporation, v is the wind speed, q_s is the saturation specific humidity evaluated at the model SST, and q_a is the air humidity. Away from coasts atmospheric boundary-layer processes, evaporation, and convection bring the air humidity into an approximate equilibrium with the underlying SST such that there is a close relationship between the two (e.g., Betts and Ridgeway 1989). Hence to specify q_a from data imposes a constraint on the model SST that forces it toward the observed SST and that we wish to avoid. SZC assumed that q_a was a fixed proportion of q_s, which assumes a near-constant relative humidity. However, the observed relative humidity is seen to vary over the tropical Pacific and tends to be higher over the cold water and lower over the warm water. This has been explained by variations in atmospheric boundary layer depth since a deeper, more turbulent, boundary layer is more effective at mixing moisture upward and away from the surface (Betts and Ridgway 1989; Wallace et al. 1989). As SST increases, q_a increases, but the relative humidity decreases. This suggests the relation

$$q_a = a + bT_s, \qquad (3)$$

where T_s is the SST in °C. With this form q_a increases with SST but less rapidly than the exponential increase of q_s. The coefficients a and b were found by fitting this formula to the monthly mean climatological values given by Weare et al. (1980). The relationship explains 91% of the variance of q_a.

The sensible heat flux is also calculated with a standard bulk formula:

$$Q_{\text{SH}} = \rho_a c_E c_p v (T_s - T_a), \qquad (4)$$

where c_p is the specific heat capacity of water and T_a is the air temperature. Air temperature, like air humidity, closely tracks the SST and again cannot be specified externally without imposing an undesired constraint on the model SST. We model T_a as

$$T_a = T_s - c. \qquad (5)$$

Hence the spatial pattern of the sensible heat loss is the same as that of the wind speed. While this is not exactly correct, the magnitude of this term is typically less than 10% of either the latent or solar radiation terms and so this is not of immediate concern. The longwave formula used follows Berliand and Berliand

(1952): Godfrey et al. (1991) show that it quite successfully reproduces the measured longwave flux over the west Pacific:

$$Q_{LW} = \epsilon\sigma T_s^4(f_1 - f_2 e^{1/2})(1 - a_{out}C^2) + 4\epsilon\sigma T_s^3(T_s - T_a). \quad (6)$$

In Eq. (6) ϵ is the emissivity of seawater (0.97), σ is the Stefan–Boltzmann constant, e is the surface vapor pressure ($p_s \times q_a/0.622$ with p_s the surface pressure that is assumed to be a constant 1000 mb), and C is the cloud cover fraction. Here f_1 and f_2 are parameters commonly taken to be 0.39 and 0.05, respectively. Here a_{out} accounts for the reduction of net outgoing longwave radiation by cloud cover. The cloud cover fraction is taken from ISCCP data.

The above heat flux formulation includes a number of empirical parameters that are inadequately known from data but that effect the magnitude and pattern of the surface heat flux. These are the exchange coefficient, c_E; the factors f_1, f_2 in the longwave formula; the parameters a and b governing the modeled air humidity; and the air–sea temperature difference c. Here a_{out} is generally taken to be dependent on the height or type of cloud cover (Weare et al. 1980) or latitude (Esbensen and Kushnir 1981). Physically, as the cloud base height increases, the cloud radiates downward at a colder temperature so the net upward flux at the surface *increases*. Fung et al. (1984) confirmed this behavior in a radiative transfer model. In terms of the cloudiness parameter, a_{out} should decrease with increasing cloud base height. Fu et al. (1990, Fig. 11) show how observed convective cloud top temperature decreases (or cloud top height increases) with increasing SST. They also show that deep convective clouds are favored by higher SSTs. Graham and Barnett (1987) have shown that deep convection tends to favor water warmer than 28°C. These results suggest that in areas of high SST the clouds most affecting the surface longwave radiation will be the high cirrus anvils associated with deep convection (Ramanathan and Collins 1991). In contrast, in colder regions of the oceans cloud cover is dominated by trade cumulus or marine stratocumulus with low cloud base (Albrecht et al. 1985). To account for this distinction as simply as possible we take a_{out} to be 0.4 if the SST exceeds 28°C and 0.8 otherwise.

The optimization of the surface heat flux model described in the next section will seek to alter the adjustable parameters within prescribed limits in order to provide the best possible fit between observed and modeled SST. The step function dependence of a_{out} on SST makes this parameter difficult to optimize. Initially we used a constant value of a_{out} and included it in the optimization but modification of its value improved the SST very little. Slightly better results were obtained with the step function dependence that supports the physical validity of this form. We hence decided to leave a_{out} fixed as a step function and optimize the other uncertain parameters within the longwave formula.

4. Methodology for optimization of surface heat flux parameters

The methodology for establishing the best fit heat flux parameters is described in detail in BC. First an a priori set of parameters is chosen. The model is spun up and then forced with FSU winds and either the ERBE or ISCCP solar radiative forcing climatology and integrated to equilibrium. At each time step the residual heat flux needed to bring the model SST into agreement with the Climate Analysis Center (CAC) observed SST (Reynolds 1988) is computed. An optimization calculation is then performed that varies the uncertain parameters within the SST calculation in an attempt to minimize the residual flux. Most of the uncertain parameters are within the surface heat flux model but the drag coefficient, C_D, is also included since variations in this will alter the advection of SST. Also included is a parameter, γ, governing the efficiency of entrainment of water into the mixed layer (see SZC and BC). The optimization provides a new set of parameters and their standard error. If the standard error of the optimized parameter equals, or exceeds, that of the a priori parameter, then the parameter is poorly resolved. Only parameters that are well resolved are ultimately changed in the model.

To perform the optimization we must assign uncertainties to each of the model parameters and to the forcing data. We assume that each parameter is possibly in error to within 30%. The longwave flux is quite sensitive to the combined effect of small changes in f_1 and f_2, so these were constrained to vary by no more than 15%. The optimization is not allowed to change the parameters by more than these amounts. Since the easiest error for the optimization routine to remove is a uniform offset between model and observed SST, and since the principal difference between the two solar radiation datasets is of this nature, we assume the uncertainty in the solar flux is given by the deviation around this mean difference. The standard deviation of the differences between 20°N and 20°S is of order 5 W m^{-2}. The main additional uncertainty in the heat flux comes from the latent heat flux term. The standard deviation of the difference between the modeled and observed q_a is about 0.7 g kg^{-1}, which corresponds to an uncertainty of about 20–30 W m^{-2} in the latent heat flux. In low wind speed areas the (absolutely necessary) assumption of a minimum wind speed in the flux formula is likely to introduce errors of about the same amount. Uncertainties in the other two terms will be smaller. To some extent the errors introduced by these uncertainties are self correcting since large SST errors will introduce compensating fluxes. We choose, perhaps conservatively, 30 W m^{-2} to characterize the overall uncertainty in the heat

flux. Differences between model and observed SSTs that can be accounted for by corrective heat fluxes of this order or smaller cannot be used to identify model errors.

It was soon discovered that the largest model-data differences occur in upwelling regions where small changes to the heat flux parameters are incapable of removing dynamical model errors. Hence to give the optimization procedure the best opportunity to remove errors introduced by heat flux uncertainties the optimization was only performed on model data west of 120°W.

The model is then run with the new set of parameters and the SST computed. Since the new parameters are as physically reasonable as the a priori set, this SST is the best the model can reproduce for a justifiable choice of model parameters. Remaining differences with observations are due to inadequacies of the dynamical or heat flux models or due to errors in the forcing data (solar radiation, cloud cover, and winds) or, less likely, errors in the observed SST. If the remaining differences are sufficiently small that they can be accounted for by uncertainties in the forcing data, then the ocean model cannot be unambiguously demonstrated to be wrong and it must be considered successful. If, however, the errors are too large to be accounted for by data uncertainties, then it is unambiguously demonstrated that the model is inadequate for its chosen task since no reasonable choice of model parameters is capable of bringing observed and modeled SST into acceptable agreement.

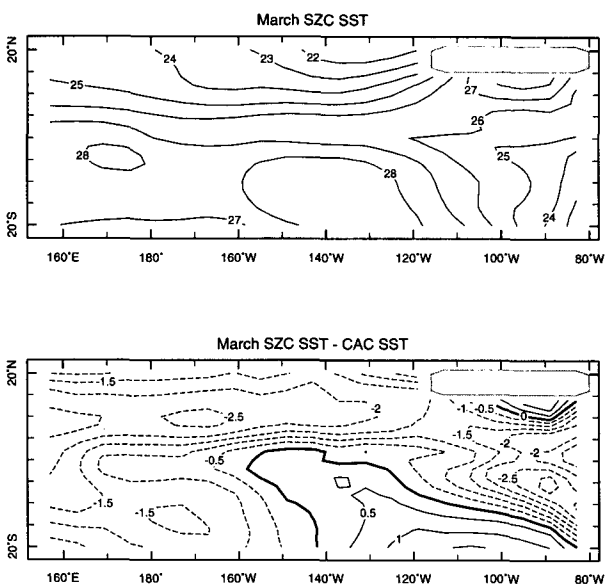

FIG. 4. (a) Modeled SST (°C) with the Seager et al. (1988) surface heat flux for March. (b) Model SST minus CAC observed SST (°C) for March.

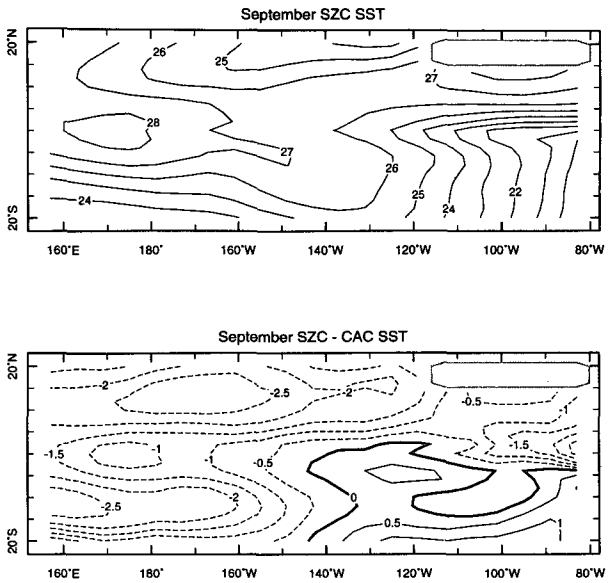

FIG. 5. Same as Fig. 4 but for September.

5. Model results

a. *SZC heat flux formulation*

As a benchmark case we present the SSTs obtained using the surface heat flux formulation of SZC and BC. This uses the solar heat flux formula of Reed (1977) together with the ship-observed cloud cover of Weare et al. (1980), assumes that the air humidity is a fixed proportion of the saturation humidity at the SST, and combines the sensible and longwave heat losses into a single Newtonian cooling term proportional to the SST in degrees centigrade. The parameter values used by the model were those given in SZC except here the minimum wind speed used in the latent heat flux is 5 m s^{-1} rather than 4 m s^{-1}. Assumption of a minimum wind speed is necessary for two reasons. First, although we assume a constant exchange coefficient, detailed flux parameterizations indicate the coefficient increases at low wind speed conditions (e.g., Liu et al. 1979). Second the wind speed we use is inverted from the FSU pseudostresses. This probably underestimates the mean wind speed because of undersampling and averaging of high-frequency wind fluctuations. Also, in SZC the SST calculation was done on a coarser grid than that used here. No tuning of the parameters was performed (BC showed tuning did little to improve the Pacific simulation with this heat flux formulation). The model was integrated with seasonally varying climatological forcings until a steady seasonal cycle was simulated. The results shown are for the last year of the run.

The model SST and differences, model minus CAC, are shown in Fig. 4 for March and in Fig. 5 for September. The most obvious model errors are the year-

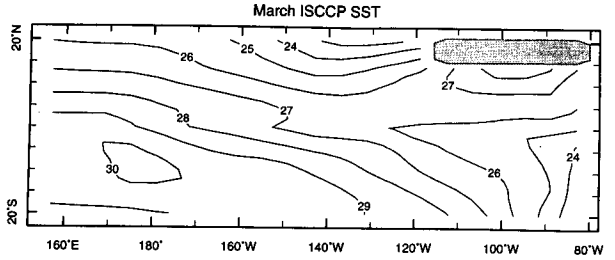

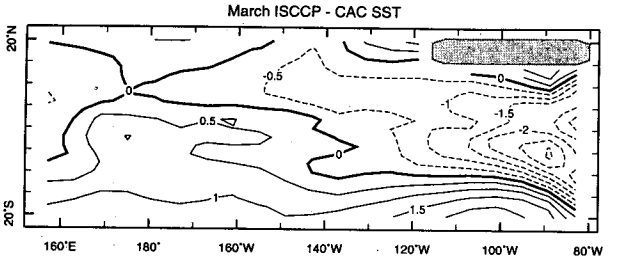

FIG. 6. (a) Modeled SST (°C) with the ISCCP surface solar radiation for March. (b) Model SST minus CAC observed SST (°C) for March.

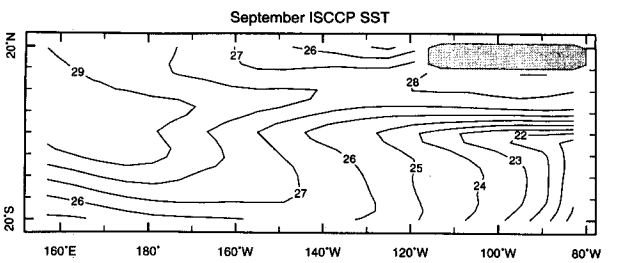

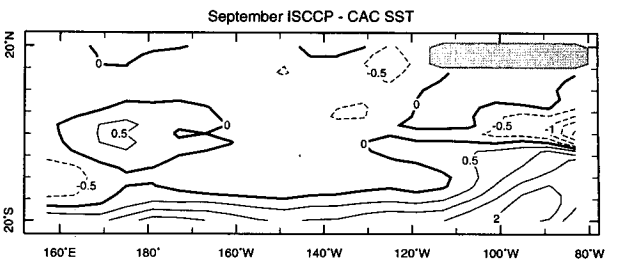

FIG. 7. Same as Fig. 6 but for September.

round underestimation of SST north of the equator and south of the equator in the western half of the basin and the overestimation south of the equator in the eastern half. In addition there is a seasonal error with the model being too cold off the South American coast from December through May. Errors in all these regions often exceed 2°C. Blumenthal and Cane found that with this heat flux formulation, optimization of the uncertain parameters did not greatly improve the simulation.

b. ISCCP and ERBE solar radiation data and the new heat flux formulation

In this case we use the more complete heat flux formulation described in section 3b together with either the ISCCP downward solar radiation adjusted for the surface albedo or the ERBE net surface solar radiation. For both cases ISCCP-derived cloud cover is used in the longwave formula. The model was forced with the seasonally varying climatological solar forcing and integrated until a steady seasonal cycle was obtained. The climatology was defined over the five years 1985–1989 to conform to the shorter period of the ERBE data. Results shown are for the last simulated year of each experiment.

For the ISCCP case, the simulated SSTs and differences, model minus CAC, are shown for March in Fig. 6 and for September in Fig. 7. In this case the heat flux parameters are chosen by optimization and are shown in Table 1 together with the a priori values. The corresponding quantities for the case with ERBE data are shown in Figs. 8 and 9 and the parameters used are also given in Table 1. Since the two simulations are quite similar we will discuss the results together. The most notable feature of these simulations compared to the simulation with the SZC parameterization is the reduction of the size of the systematic and persistent errors in almost all the open-ocean regions. The model no longer underestimates the off-equatorial SST. The main error away from the eastern boundary is that the model is persistently too warm south of about 10°S. There is no counterpart of this error to the north of the equator. In addition, in the early part of the year (e.g., March) the model is too cold under the eastern Pacific intertropical convergence zone (ITCZ). The size of these errors is considerably smaller than the off-equatorial errors in the case with the SZC flux formulation. Away from the east coast, systematic and persistent errors have been reduced as a consequence of introduction of the satellite solar forcing. The simulations, however, reveal the major model flaw: persistent overestimation of the model SST off the South American coast from April through July (not shown,

TABLE 1. The a priori parameter values and the optimized values used in the simulations using the ISCCP and ERBE solar radiation data.

	a priori	ISCCP	ERBE
C_D	0.0016	0.0016	0.0016
C_E	0.0015	0.0013	0.00124
a	−9.42	−9.42	−9.42
b	0.97	0.97	0.97
c	1.0	0.835	0.71
f_1	0.39	0.416	0.417
f_2	0.05	0.0485	0.0486
γ	0.5	0.383	0.383

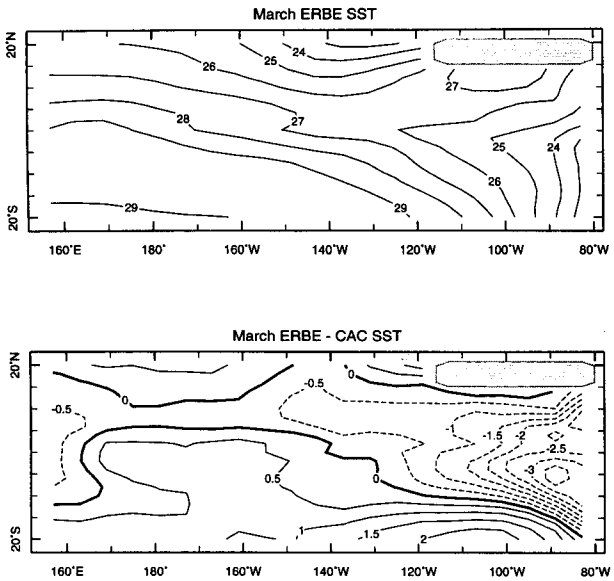

FIG. 8. (a) Modeled SST (°C) with the ERBE surface solar radiation for March. (b) Model SST minus CAC observed SST (°C) for March.

but see section 6 below) where the error is of order 1.5°C. From August through March, as for the SZC model, the simulated SST in this region is too cold and the error can reach 3°C right by the coast. Clearly the introduction of satellite solar forcing has done rather little to improve the SST simulation in these eastern coastal regions.

6. Analysis of SST simulations

The results in the previous section have shown significant changes in the SST simulation as a result of use of satellite-derived solar radiative forcing and a new heat flux parameterization. In this section we will attempt to explain these differences and try to answer the fundamental question: Does inclusion of the new forcing data allow us to unambiguously identify model inadequacies?

The most notable improvement of this model over the earlier ones of SZC and BC is the elimination of the persistent cold waters north and south of the equator. In SZC it was stated that an early look at ISCCP results showed the tropical cloud cover to be more spatially variable than ship data indicated. They argued inclusion of this effect would warm the off-equatorial areas of limited cloud cover. The results presented here confirm this. Comparison of the Weare et al. (1980) solar radiative forcing with that derived from ISCCP show that in these regions the ISCCP data is consistently 20 W m^{-2} or so higher, which is clearly responsible for warming the waters in these regions. SZC also expected the satellite solar radiation over the warm pool to be less than the Weare et al. estimates and that this would cool the western Pacific where the model was too warm. This turns out to not be the case since the satellite solar in this region is in fact either about the same (ERBE) or actually higher (ISCCP) than Weare et al.'s (1980). However, the model SST is only slightly too warm in this region, so the extra solar radiative heating has been balanced by increased cooling. The increased cooling is due to the longwave flux that exceeds the 45 W m^{-2} combined sensible plus longwave heat loss SZC had in this region and to the increased latent heat loss from the 1 m s^{-1} higher minimum wind speed. The latter compensates for the lower wind speeds inverted from the FSU pseudo stresses compared with the directly observed wind speeds reported by Weare et al. (1980).

Despite the ISCCP data giving a net solar radiation receipt some 18 W m^{-2} larger than the ERBE data, the simulations with the two datasets are very similar both in pattern and the basin mean temperature. The tuning procedure primarily compensates for the greater ISCCP solar receipt by increasing the upward longwave radiative loss. This can reach 90 W m^{-2} in areas of clear skies, considerably higher than in previous estimates. In contrast the simulations with ERBE data have longwave radiative losses that are typically 10 W m^{-2} less than in the ISCCP case. The remainder of the difference between the ISCCP and ERBE simulations is made up by a latent heat loss in the ISCCP case that is some 8 W m^{-2} higher.

The spatial patterns of the modeled fluxes with ISCCP forcing are shown in Figs. 10 and 11 for March and September. The latent and sensible heat fluxes have the familiar patterns with maximum fluxes in the core of the trades where the wind is strong and minimums over the eastern cold tongue. In the western Pacific the minimum is less marked because of the application of

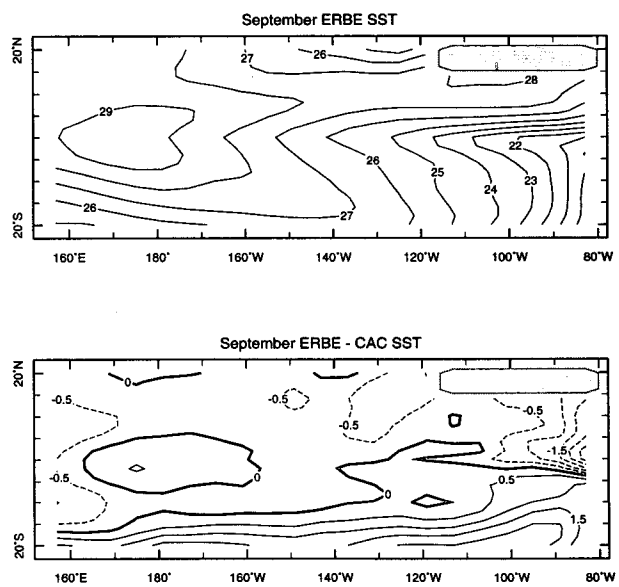

FIG. 9. Same as Fig. 8 for September.

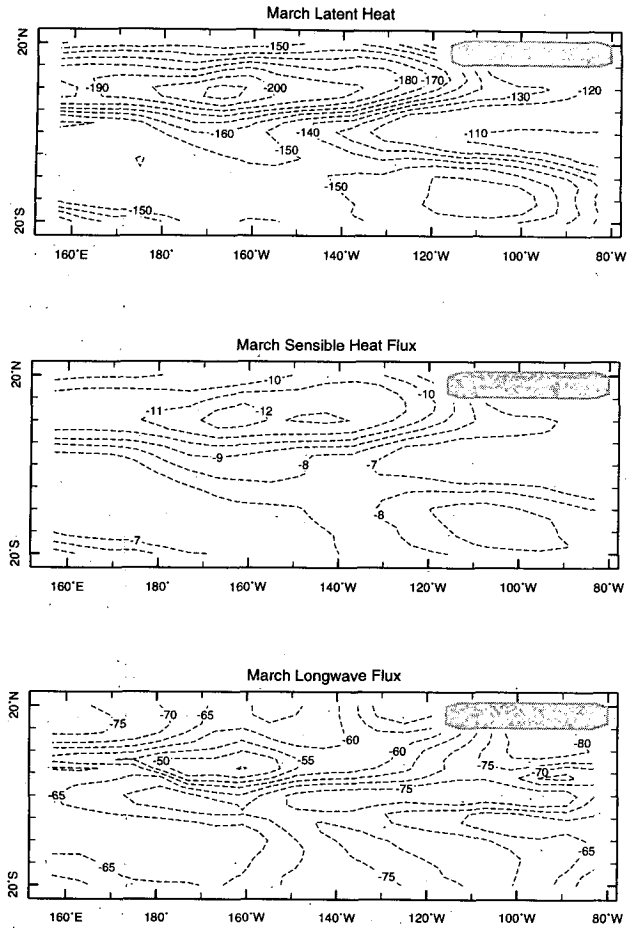

FIG. 10. The latent, sensible, and longwave fluxes in W m^{-2} for March and the case with ISCCP solar forcing.

the minimum wind speed condition and fluxes here are 20–30 W m^{-2} higher than in the atlas of Weare et al. (1980). As observed the sensible heat flux is small compared to the latent heat flux. The longwave fluxes (Figs. 10c and 11c) also show the typical pattern of maximizing in clear sky regions and being lower in cloudy regions of the west Pacific and the ITCZ.

Recent work suggests that the longwave cooling may indeed be higher than the estimates to be found in the atlases of Weare et al. (1980) and Esbensen and Kushnir (1981). Godfrey et al. (1991) reported outgoing longwave fluxes over the west Pacific of 60 W m^{-2}. Chou (1991) used the ISCCP radiance data and a cloud scheme to infer surface radiative fluxes and found tropical west Pacific values of 30–70 W m^{-2}. The upper limits in these two studies are twice the typical values in atlas estimates. This suggests that a longwave cooling of 80 W m^{-2} in the cloud free regions of the eastern Pacific is potentially reasonable. The modeled longwave flux also has a similar magnitude and pattern to the fluxes derived through a combination of ERBE data and GCM model experiments by Harshvardhan (1992). In both the ERBE and ISCCP simulations the combined effects of the longwave and sensible cooling considerably exceed the values in SZC and BC. It appears the longwave fluxes are plausible but we believe their reliability over the entire Pacific still remains to be demonstrated.

The similarity of the two SST simulations is notable. In Figs. 11 and 12 we show the corrective heat fluxes required to bring the modeled SSTs into agreement with those observed for March and September. The contour interval is chosen to correspond to our best guess of the remaining uncertainty in the surface heat flux. Again the similarity of the patterns is striking: either the two solar radiation datasets are subject to the same errors or the error patterns are produced by model failings. That the two datasets are independent and derived using quite different algorithms suggests that there is little uncertainty in the pattern of the solar radiation receipt. Only the amplitude is seriously in question. Hence the patterns of corrective heat flux are maps of model failings.

In most open-ocean regions the size of the required corrective heat flux is of the order of the uncertainty

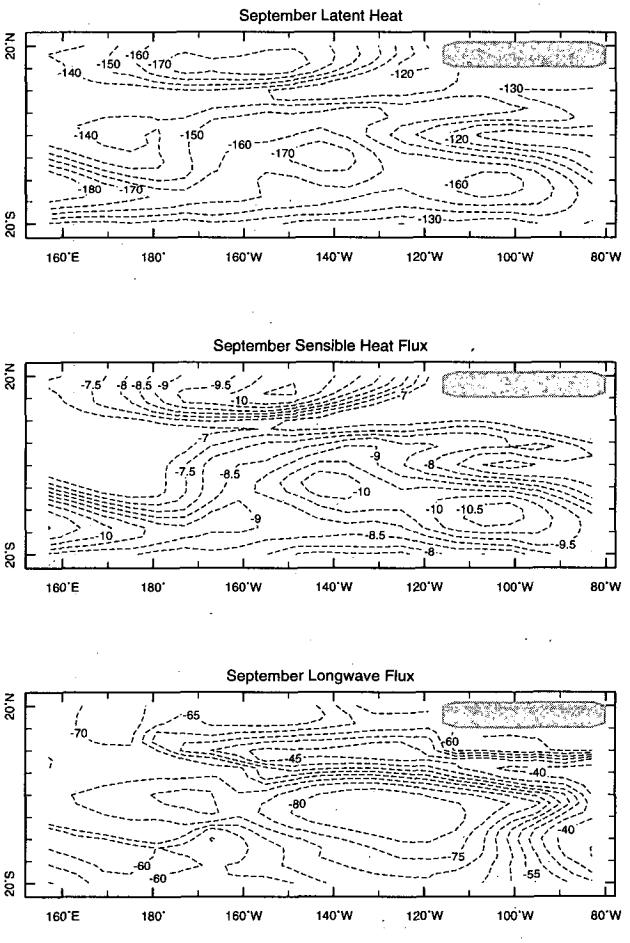

FIG. 11. Same as Fig. 10 but for September.

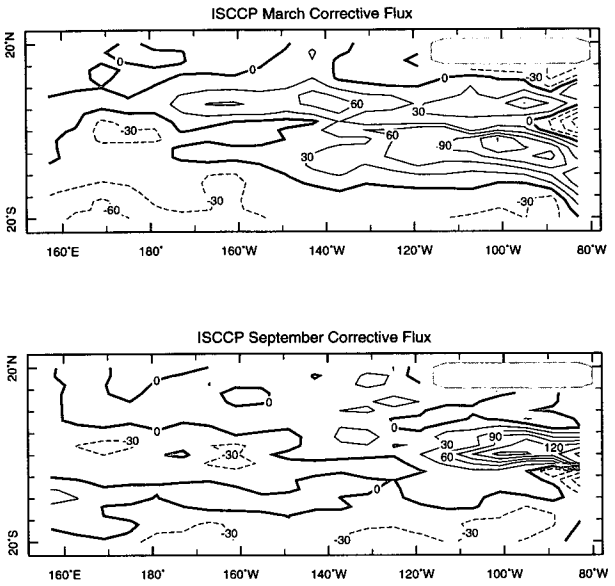

FIG. 12. The heat flux in W m^{-2} required to adjust the modeled SST to observed SST for the case with ISCCP solar forcing for (a) March and (b) September.

in the surface heat flux. The exception is that during the early part of the year the model is too cold under the central Pacific ITCZ. However, by the South American coast, and in the east Pacific upwelling zone, the model is almost always either too warm or too cold. In this area the size of the corrective heat flux greatly exceeds what can be accounted for by uncertainties in the heat flux. Model error is clearly indicated. This result is expected since it is in these regions that the linear model and mixed-layer formulation are least valid. In the open ocean the SST is primarily determined by one-dimensional processes but it is nonetheless unexpected that a constant depth mixed layer performs so well.

The seasonal cycle of equatorial SST in the model is governed in much the same way as described in SZC. Figure 14 shows longitude–time diagrams of various quantities averaged from 3°N to 3°S for the case with ISCCP forcing (the ERBE case is much the same). As observed, the seasonal cycle is pronounced in the east and almost nonexistent in the west. As the year begins the east warms until April due to increased downward heat flux (mostly due to increasing solar radiation). Cooling begins after April as the surface heat flux decreases and, later in the year, as upwelling significantly cools the surface. The coldest temperature is reached in October. The cooling due to horizontal advection is also large. In the east, cold equatorial waters are advected away from the equator, whereas farther west advection of cold waters from the east dominates. During the coldest time of the year, the meridional SST gradients are largest, and diffusion offsets some of the dynamical cooling. Diffusion is important only in the cold tongue. As the upwelling decreases and the downward surface flux increases, the model SST warms through to the end of the year. In the far west the weak seasonal cycle is determined entirely by the surface heat flux.

The apparent importance of horizontal advection in the east needs to be put into perspective. Meridional advection and upwelling both result from the seasonal variation in the wind stress. The upwelling puts in place cold water that is advected poleward to cool adjacent waters. Zonal advection similarly works on an SST gradient largely created by the upwelling in the east. Hence, in this model, the seasonal cycle in the eastern and central Pacific is dominated by the seasonal cycle in upwelling flux. The upwelling flux is influenced by the seasonal cycles in entrainment and in thermocline depth, which dictates the temperature of the water entrained. The obvious errors in the model raise questions as to whether this dominance of upwelling is correct. That the differences between the model and observed SST propagate westward, whereas no propagation is seen in the model SSTs alone, also suggests that the seasonal cycle is not being modeled correctly in this region.

7. Discussion and conclusions

The recent release of satellite-derived surface solar radiation products presents an opportunity to improve the SST simulations of global ocean models. Prior to the advent of satellite data, solar radiative forcings were derived from the calculated solar radiation at the top of the atmosphere reduced by an empirically determined factor depending on ship-observed total cloud cover. This was subject to error in the empirical rela-

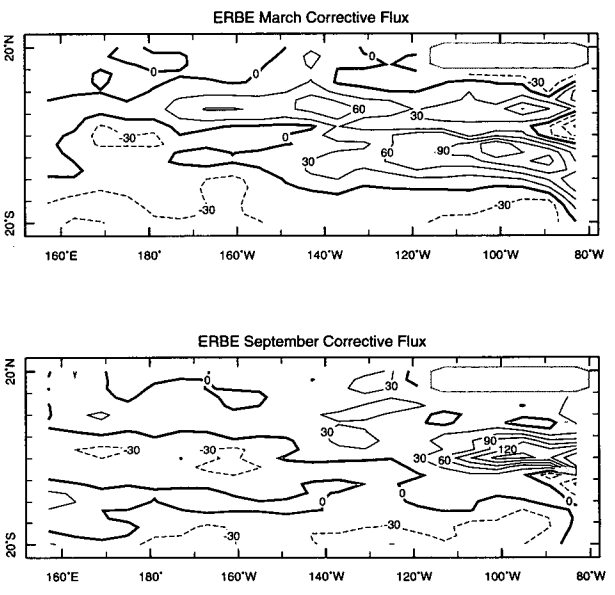

FIG. 13. Same as Fig. 10 but for case with ERBE solar forcing.

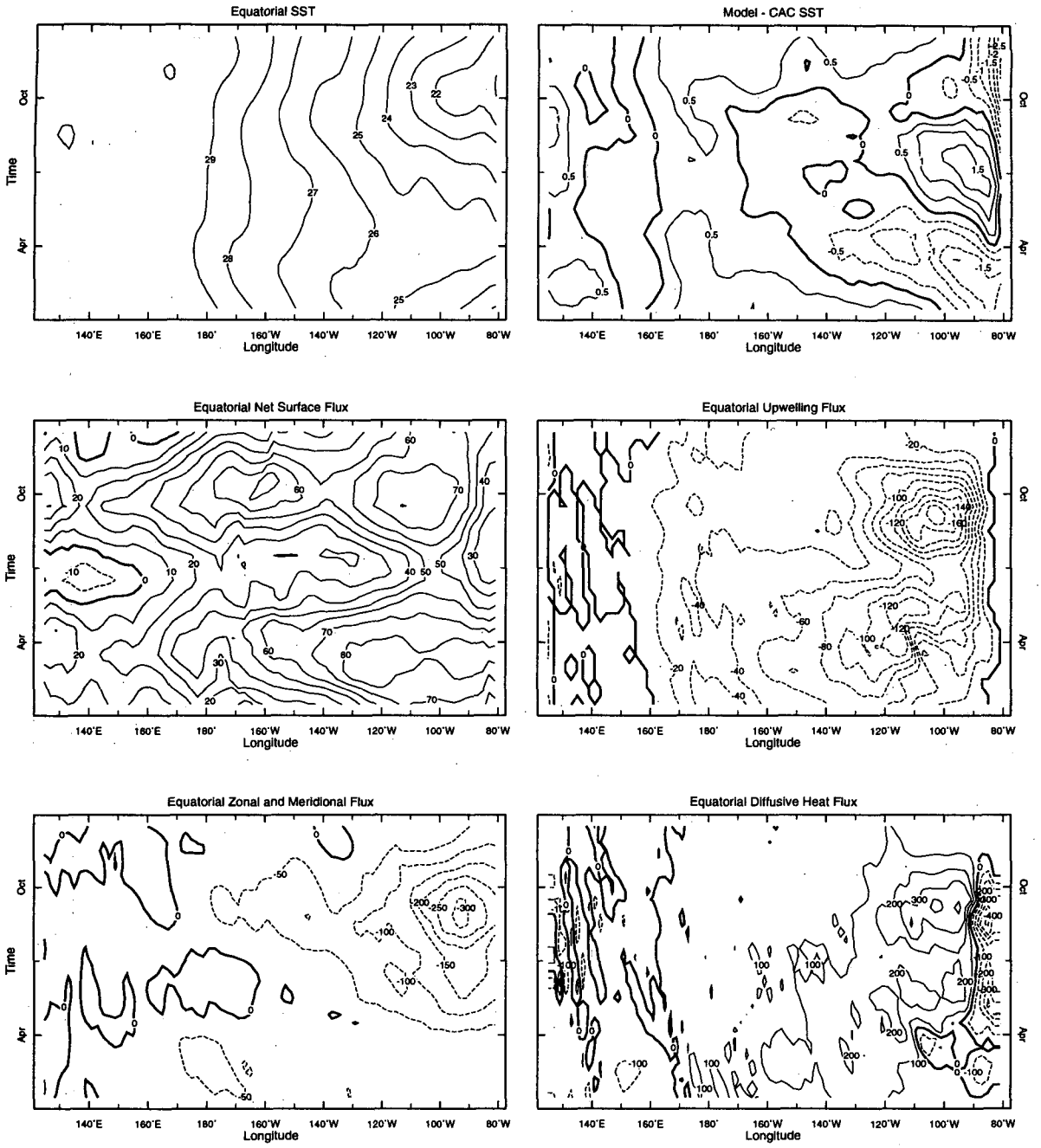

FIG. 14. Hovmoeller diagrams of the variations with longitude and time on the equator of (a) the model SST, (b) model SST minus CAC SST, (c) the net surface heat flux, (d) the upwelling flux, (e) the horizontal advective flux, and (f) diffusion for the case with ISCCP solar forcing. Temperatures are in °C and fluxes are in W m^{-2}.

tionship and in the observed cloud cover. The latter is a subjective measurement and is reported in units corresponding to 12.5% cloud cover. In the Tropics a 12.5% variation in cloud cover can translate into more than 25 W m^{-2} uncertainty in the solar flux, which would alter the temperature of a 50-m-deep layer by 1 K in 100 days. The satellite products aim to avoid these problems through use of state of the art radiative transfer algorithms to derive the surface radiation directly from the observed reflected flux at the top of the atmosphere.

We present a comparison of two independent solar radiation datasets: the ISCCP product as described by Bishop and Rossow (1991) and the Earth Radiation

Budget Experiment product as described by Li and Leighton (1993). Unfortunately the difference between these two datasets is larger than the stated goal of the WCRP Surface Radiation Budget Program of 10 W m^{-2} (Suttles and Ohring 1986). The difference is influenced by the fact that the ERBE product is the net solar radiation, whereas the ISCCP product provides the downward solar flux, which needs to be multiplied by an albedo to give the net solar radiation. However, an unreasonably large albedo would be required to convert the ISCCP downward solar radiation into a net flux comparable to the ERBE data. Both datasets have been calibrated against ground truth data although not in the same places and only in mid to high latitudes.

While these differences are superficially discouraging, the differences between these two datasets are dominated by an offset with ISCCP values higher than ERBE values. The spatial patterns within the two datasets are very similar despite the very different algorithms used to derive the radiation at the surface. In the tropical Pacific region, which is our main focus, the differences that remain after removal of the mean offset are clearly correlated with cloud cover: the ISCCP surface solar radiation has a larger variation with cloud cover than the ERBE data. The differences introduce a scatter of only ± 5 W m^{-2}. Overall the dominance of the offset, the small scatter around it, and the correlation of that scatter with cloud cover suggest that reconciling the two datasets will be relatively easy.

We present the first simulation of SST that we are aware of that uses these satellite solar radiation products. Our goal is twofold: to improve the SST simulations begun by Seager et al. (1988) and continued by Seager (1989) and Blumenthal and Cane (1989), and to use the reduced uncertainty in the modeled heat flux in an attempt to more clearly identify dynamical model failings. We continue the methodology of heat flux formulation that avoids specifying atmospheric quantities over which the ocean has direct control such as air temperature and humidity. To specify these is to put in much of the answer: it improves the SST simulation by forcing the fluxes toward those required to get the SST right. This leads to errors in the feedback between the SST and the fluxes and alters model sensitivity. It is not the right procedure to use when attempting to locate model failings: since the SST is being forced toward observed it is not possible to distinguish errors caused by the ocean model from those caused by the flux formulation.

We instead adopt the method of optimization of heat flux parameters introduced by Blumenthal and Cane (1989). This alters the uncertain parameters in the heat flux formulation within reasonable ranges to find the set that leads to the best possible SST simulation. The optimized set of heat flux parameters is as justifiable as any other commonly used. However, if differences between the model and observed SST are now larger than can be accounted for by the residual uncertainty in the heat flux, the ocean model is unambiguously demonstrated to be in error. Rather than fixing the fluxes in order to get the SST correct at all costs, this methodology allows identification of model errors and acts to guide efforts at model improvement.

We present three SST simulations. The first is intended to be a reference point and uses the simplified heat flux formulation of Seager et al. (1988) (including the solar term) together with ship-observed cloud cover of Weare et al. (1980). The SST simulation was seen to be too cold in most off-equatorial regions but too warm south of the equator in the east and to also have a seasonal error in the coastal upwelling region. In many regions the errors reached 2°C. Blumenthal and Cane (1989) argued this level of error was at the limit of what could be accounted for by heat flux uncertainty. We then present two simulations with the satellite solar radiation datasets. These simulations include a more complete heat flux formulation that takes into account separately the longwave and sensible heat flux and introduces a simple parameterization of the air humidity in terms of the modeled SST. One of the main effects of the satellite-derived solar radiation data is a warming of the off-equatorial SSTs where the satellite data shows more solar radiation receipt than is given by the Reed (1977) formulation with ship observed clouds. The SSTs simulated with the two datasets are very similar despite the approximately 18 W m^{-2} offset between the two. The optimization procedure alters the heat flux parameters to compensate for the differences. The larger net solar flux given by the ISCCP data is balanced by larger longwave and latent heat losses. In these simulations the longwave losses considerably exceed those given in atlas estimates, in accord with recent theoretical and observational estimates of their correct size. This suggests the longwave flux is not of negligible importance to the net surface flux. It also cannot be parameterized in terms of SST alone (as SZC and BC tried) and is better treated in a manner analogous to that used here, or with a full radiative transfer calculation.

Clear differences remain between the modeled and observed SST. The most obvious errors are in the upwelling region in the east and along the South American coast where the model is generally too cold August to March and too warm April to July. The model is also too cold in the ITCZ region of the east and central Pacific from November to May and generally too warm south of about 10°S. Elsewhere the differences between model and observed SST can be accounted for by corrective heat fluxes of the order of the remaining uncertainty in the surface heat flux. Hence in these regions we cannot prove the ocean model is in error although it almost certainly is. In contrast, in the upwelling regions optimization of the heat flux parameters does little to reduce discrepancies between the model and data. This is saying that in this region *no reasonable*

surface heat flux will lead to an acceptable SST simulation. In other words, our methodology indicates unambiguously that the dynamical model is in error in this region. The optimization procedure has isolated the regions of the ocean where ocean dynamics (and mixing) contributes most to the SST as those regions where the ocean model is in error. Where the heat flux is the dominant process we are unable to determine model errors.

The errors in the upwelling region affect the strength and phase of the seasonal cycle. As the eastern Pacific SST warms in the early part of the year, the model needs a positive corrective heat flux. As it cools after Northern Hemisphere spring, it needs a negative corrective heat flux. The errors correlate with the difference between the SST and the temperature of the subsurface water available for entrainment into the mixed layer. If this difference is large, the model needs an extra addition of heat to bring the SST into line. If it is small, the model needs an extra extraction of heat. The problem could be that the annual cycle in upwelling is in error, for example. However, although the upwelling is calculated from a simple frictional momentum balance in the mixed layer, we feel this is a reliable part of the model. It could instead be due to a poor simulation of the temperature of water available to be upwelled. However, comparison of that temperature (which in the model is actually parameterized in terms of the thermocline depth) with the observations given by Levitus (1982) shows this simulation to be quite accurate. This suggests that the problem instead lies in the parameterization of entrainment.

The assumption of a constant depth mixed layer in the model dictates that the entrainment must balance the upwelling at the base of the mixed layer. In nature mixed-layer divergence could instead be balanced by a shallowing of the mixed-layer depth in the absence of entrainment or a combination of the two. This is most likely to occur if the temperature jump between the mixed layer and the water below is large since then the energy input from the wind may be insufficient to lift cold dense water from below into the mixed layer. When the temperature discontinuity at the mixed-layer base is small, entrainment should be more efficient and the mixed layer is likely to deepen. We feel that exclusion of this process in our model is the most likely cause of the errors we have identified. For example, in the early part of the year the model upwelling is strong in the east Pacific and the model is too cold. However, during this time the temperature discontinuity at the base of the mixed layer becomes large (up to 8°C) and this should inhibit entrainment, reducing the surface cooling associated with vertical motion.

This work reports on ongoing efforts made at Lamont-Doherty Earth Observatory to model the total SSTs of the tropical oceans using fairly simple ocean models. The goal is to understand the seasonal cycle and its interactions with interannual variability and to develop coupled atmosphere–ocean models that simulate both of these phenomena rather than needing to specify the mean seasonal cycle. Although progress in modeling total SST was rapid early on, we soon realized that uncertainties in the forcing data (and especially the solar radiative forcing) were so large that they made it difficult to identify model errors. Now that satellite surface solar radiation data have become available, we feel this frustrating stage has been overcome. We interpret the ability to produce two very similar SST simulations with two independent solar radiative datasets as indicating that the uncertainties in the solar radiative forcing have been reduced. In the process we have identified a fundamental model error: an overly simple treatment of entrainment of water into the mixed layer in upwelling regions. It may be argued that we could have identified that before but these regions are also regions of extensive low-level cloud cover and sparse ship observations, so we could never rule out errors in the solar radiation. We believe that is now a lot less likely. Interest in the seasonal cycle makes it increasingly necessary to improve the mixed-layer/entrainment parameterizations in ocean models in order to guarantee satisfactory progress.

Acknowledgments. We wish to thank Mark Cane for valuable discussions relating to this work, Zhanqing Li for provision of the ERBE data, and Jim Bishop and Bill Rossow for essential guidance with the ISCCP data. RS was supported as a NOAA Program in Climate and Global Change Visiting Postdoctoral Fellow. MBB was supported by National Aeronautics and Space Administration Grant NAGW-916. The production of the ISCCP dataset was supported by National Aeronautics and Space Administration Grant NAGW-2189 (J. K. B. Bishop, Principal Investigator).

REFERENCES

Albrecht, B. A., R. Penc, and W. H. Schubert, 1985: An observational study of cloud-topped mixed layers. *J. Atmos. Sci.*, **42,** 800–822.

Berliand, M. E., and T. G. Berliand, 1952: Determining the net longwave radiation of the earth with consideration of the effect of cloudiness (in Russian). Tech. Rep. 1, Izv. Akad. Nauk. SSSR Ser. Geofiz., 63 pp.

Betts, A. K., and W. Ridgway, 1989: Climatic equilibrium of the atmospheric convective boundary layer over a tropical ocean. *J. Atmos. Sci.*, **46,** 2621–2641.

Bishop, J. K. B., and W. B. Rossow, 1991: Spatial and temporal variability of global surface solar irradiance. *J. Geophys. Res.*, **96,** 16 839–16 858.

Blumenthal, M. B., and M. A. Cane, 1989: Accounting for parameter uncertainties in model verification: An illustration with tropical sea surface temperature. *J. Phys. Oceanogr.*, **19,** 815–830.

Cane, M. A., 1979: The response of an equatorial ocean to simple wind stress patterns II: Numerical results. *J. Mar. Res.*, **37,** 355–398.

——, 1984: Modeling sea level during El Niño. *J. Phys. Oceanogr.*, **14,** 586–606.

——, 1991: Forecasting El Niño with a geophysical model. *Teleconnections Linking Worldwide Climate Anomalies,* M. Glantz, R.

Katz, and N. Nicholls, Eds., Cambridge University Press, 345–369.

——, and R. Patton, 1984: A numerical model for low-frequency equatorial dynamics. *J. Phys. Oceanogr.*, **14**, 1853–1863.

Chou, M.-D., 1991: The derivation of cloud parameters from satellite-measured radiances for use in surface radiation calculations. *J. Atmos. Sci.*, **48**, 1549–1559.

Cox, C., and W. Munk, 1956: Slopes of the sea surface deduced from photographs of the sun glitter. *Bull. Scripps Inst. Oceanogr.*, **6**, 401–488.

Esbensen, S., and Y. Kushnir, 1981: The heat budget of the global ocean: An atlas based on estimates from surface marine observations. Tech. Rep. 29, Climate Research Institute, Oregon State University, 27 pp.

Fu, R., A. D. delGenio, and W. B. Rossow, 1990: Behavior of deep convective clouds in the tropical Pacific deduced from ISCCP radiances. *J. Climate*, **3**, 1129–1152.

Fung, I., D. Harrison, and A. Lacis, 1984: On the variability of the net longwave radiation at the ocean surface. *Rev. Geophys. Space Phys.*, **22**, 177–193.

Geisler, J. E., M. L. Blackmon, G. T. Bates, and S. Muñoz, 1985: Sensitivity of January climate response to the magnitude and position of equatorial Pacific sea surface temperature anomalies. *J. Atmos. Sci.*, **42**, 1037–1049.

Gent, P., 1991: The heat budget of the TOGA COARE domain in an ocean model. *J. Geophys. Res.*, **96**, 3323–3330.

Godfrey, J. S., M. Nunez, E. F. Bradley, P. A. Coppin, and E. J. Lindstrom, 1991: On the net surface heat flux into the western equatorial Pacific. *J. Geophys. Res.*, **96**, 3391–3400.

Goldenberg, S., and J. O'Brien, 1981: Time and space variability of tropical Pacific wind stress. *Mon. Wea. Rev.*, **109**, 1190–1205.

Gordon, C., and R. Corry, 1991: A model simulation of the seasonal cycle in the tropical Pacific using climatological and modelled forcing. *J. Geophys. Res.*, **96**, 847–868.

Graham, N., and T. Barnett, 1987: Sea surface temperature, surface wind divergence, and convection over tropical oceans. *Science*, **238**, 657–659.

Han, Y., 1984: A numerical world ocean general circulation model, II: A baroclinic experiment. *Dyn. Atmos. Oceans*, **8**, 141–172.

Haney, R. L., 1971: Surface thermal boundary conditions for ocean circulation models. *J. Phys. Oceanogr.*, **1**, 241–248.

Harrison, D. E., 1991: Equatorial sea surface temperature sensitivity to net surface heat flux: Some ocean circulation model results. *J. Climate*, **5**, 539–549.

Harshvardhan, 1992: The use of TOA cloud longwave radiative forcing to estimate mean monthly surface longwave radiation. Hydrology and surface radiation in atmospheric models. WCRP Report No. 75, WMO/TD-492, 98 pp.

Latif, M., 1987: Tropical ocean circulation experiments. *J. Phys. Oceanogr.*, **17**, 246–263.

Levitus, S. E., 1982: *Climatological Atlas of the World Ocean.* NOAA Prof. Paper 13, U.S. Govt. Printing Office, Washington, DC., 173 pp.

Li, Z., and H. G. Leighton, 1993: Global climatologies of the solar radiation budgets at the surface and in the atmosphere from 5 years of ERBE data. *J. Geophys. Res.*, **98**, 4919–4930.

——, ——, and R. D. Cess, 1993a: Surface net solar radiation estimated from satellite measurements: Comparison with tower observations. *J. Climate*, **6**, 1764–1772.

——, ——, K. Masuda, and T. Takashima, 1993b: Estimation of SW flux absorbed at the surface from TOA reflected flux. *J. Climate*, **6**, 317–330.

Liu, W. T., K. B. Katsaros, and J. A. Businger, 1979: Bulk parameterization of air–sea exchange of heat and water vapor including molecular constraints at the interface. *J. Atmos. Sci.*, **36**, 1722–1735.

Miller, A. J., J. F. Oberhuber, N. E. Graham, and T. P. Barnett, 1992: Tropical Pacific ocean response to observed winds in a layered general circulation model. *J. Geophys. Res.*, **97**, 7317–7340.

Moura, A. D., and J. Shukla, 1981: On the dynamics of droughts in northeast Brazil: Observations, theory, and numerical experiments with a general circulation model. *J. Atmos. Sci.*, **38**, 2653–2675.

Palmer, T. N., Č. Branković, P. Viterbo, and M. J. Miller, 1992: Modeling interannual variations of summer monsoons. *J. Climate*, **5**, 399–417.

Philander, S. G. H., and A. D. Siegel, 1985: Simulation of the El Niño of 1982–1983. *Coupled Ocean-Atmosphere Models*, J. C. J. Nihoul, Ed., Elsevier, 517–541.

Ramanathan, V., and W. Collins, 1991: Thermodynamic regulation of ocean warming by cirrus clouds deduced from observations of the 1987 El Niño. *Nature*, **351**, 27–32.

Reed, R. K., 1977: On estimating insolation over the ocean. *J. Phys. Oceanogr.*, **7**, 482–485.

Reynolds, R. W., 1988: A real-time global sea surface temperature analysis. *J. Climate*, **1**, 75–86.

Rossow, W. B., and R. A. Schiffer, 1991: ISCCP cloud data products. *Bull. Amer. Meteor. Soc.*, **72**, 2–20.

Seager, R., 1989: Modeling tropical Pacific sea surface temperature: 1970–1987. *J. Phys. Oceanogr.*, **19**, 419–434.

——, S. E. Zebiak, and M. A. Cane, 1988: A model of the tropical Pacific sea surface temperature climatology. *J. Geophys. Res.*, **93**, 1265–1280.

Suttles, J. T., and G. Ohring, 1986: Report of the workshop on surface radiation budget for climate applications. Tech. Rep. WCP-115, World Meteorological Organization, 144 pp.

Wallace, J. M., T. P. Mitchell, and C. Deser, 1989: The influence of sea-surface temperature on surface wind in the eastern equatorial Pacific: Seasonal and interannual variability. *J. Climate*, **2**, 1492–1499.

Weare, B. C., P. T. Strub, and M. D. Samuel, 1980: Marine climate atlas of the tropical Pacific Ocean. Tech. Rep. 20, Dept. of Land, Air and Water Resources, University of California, Davis, 147 pp.

Zebiak, S. E., and M. A. Cane, 1987: A model El Niño–Southern Oscillation. *Mon. Wea. Rev.*, **115**, 2262–2278.